

# Denoising Speckle Noise in Optical Coherence Tomography Images- A Comparative Analysis

M.Nagoor Meeral<sup>1</sup>, Dr.S.Shajun Nisha<sup>2</sup>

<sup>1</sup> Reg.No:19211192282029, Research Scholar Ph.D., E-mail id:nmeeral1989@gmail.com

<sup>2</sup> Research Supervisor, Assistant Professor & Head, PG & Research Department of  
Computer Science, E-mail id:shajunnisha78@gmail.com

<sup>1,2</sup> Sadakathullah Appa College, Affiliation of Manonmaniam Sundaranar University,  
Abishekapatti, Tirunelveli, Tamil Nadu 627012, India

## Abstract

Ophthalmologists are paying more attention to optical coherence tomography (OCT), a macular screening tool for identifying early-stage retinal diseases. It is a non-invasive process that uses the interferometric principle to examine the innermost layers of retina. OCT causes a coarse speckle pattern while backscattering the light, which reduces the clarity of the image. The literature has implemented a variety of denoising techniques to eliminate speckle noise. In this study, denoising methods such the Gaussian filter, anisotropic diffusion, nonlocal means (NLM), BM3D, K-SVD, and WNNM are compared. Images from the Duke Dataset are used to analyze performance. Peak Signal To Noise Ratio (PSNR), Structural Similarity Index (SSIM), Normalized Correlation (NK), Normalized Absolute Error (NAE), and Average Difference are used to compare the quantitative results (AD). As a result, WNNM offers images of greater quality with significant SSIM and PSNR values.

Keywords:OCT, Speckle removal, Noise removal, Quality assessment metrics, Retinal disease

## I.Introduction:

OCT was introduced in 1991, which can acquire the posterior segment of the eye to diagnose macular disorders like Age related Macular Degeneration (AMD), Macular Edema (ME), Diabetic Retinopathy (DR), Choroid Neovascularization (CNV) etc. The defining features of OCT are non-invasiveness, high resolution and fast acquisition. Using low coherence interferometric property, it achieves micrometric resolution to manifest the cross sectional regions of retina [1][2]

While capturing, the backscattered light from the deeper tissues influences multiple uncorrelated particles known as speckle. Speckle is a multiplicative noise which has a dual property of signal carrying and signal degrading. The quality diminishing speckle should be differentiated and suppressed to preserve the subtle information of the retina. Many research works have been developed based on several hardware and softwares. Machine based techniques like frequency compounding, Spatial compounding and polarization techniques result in cost computation and lesser resolution [3].

Software techniques include computational algorithms to control the existence of degrading noises. A noisy image  $y$  is the composition of clean image  $x$  and some additive white gaussian noises  $v$ . It can be mathematically defined as  $y=x+v$ . At first, filtering algorithms get early attention in removing these degraded noises [4]. The most popular of them are Wiener filter [5], Gaussian filter [6], Anisotropic diffusion

filter[7], Non Local Means[8] etc. Further, model based techniques like BM3D[9], sparse representation based models like KSVD[10], LSSC[11], NCSR[12] methods are introduced. Following these, Low rank minimization methods like WNNM[13] and its improvements are proposed. These post processing methods are easy to implement and accounts considerable PSNR value.

This research study compares Gaussian filter, Anisotropic diffusion, Non Local Means(NLM), Block-matching and 3D filtering (BM3D), K means Singular Value Decomposition(K-SVD) and Weighted Nuclear Norm Minimization(WNNM) algorithm in terms of metrics like Peak Signal To Noise Ratio(PSNR), Structural Similarity Index(SSIM), Normalized Correlation(NK), Normalized Absolute Error(NAE), Average Difference(AD)[16][17][18].

### 1.2 Motivation and Justification:

Though several research works have been proposed to segment and classify OCT images. The presence of Speckle can degrade the texture information, further affecting the performance of retinal layer extraction and classification of macular pathologies. By exploring the literature, filtering algorithms and model based techniques are used in several OCT analysis by generating considerable PSNR value. Motivated by this, different denoising algorithms are attempted to compare and the results are justified using appropriate metrics.

### 1.3 Outline of the proposed work:

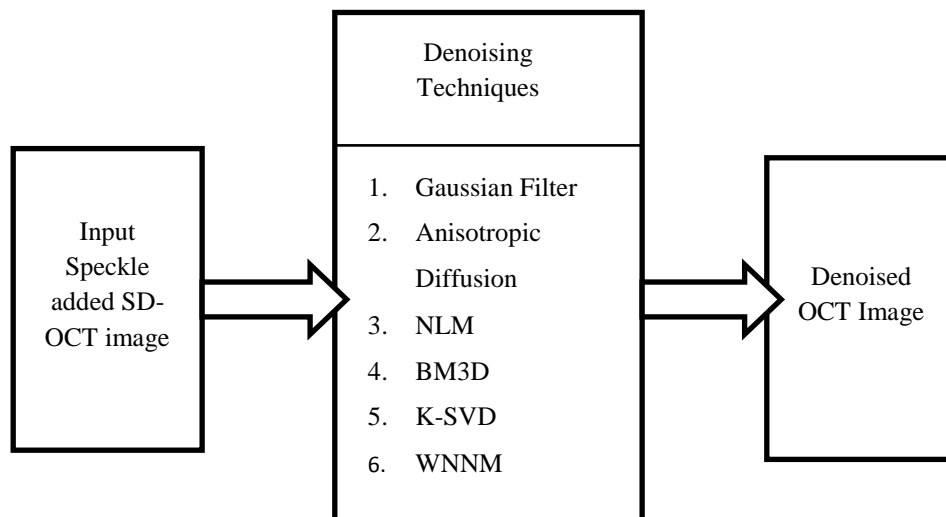


Figure 1. Outline of the proposed Work

### 1.4 Organization of the paper:

The structure of the paper is as follows. Section II includes Related Work, Section III contains methodology, Section IV provides Experimental results, Section V describes conclusion.

## II Related Work:

A diverse range of filtering algorithms are developed in the earlier decades. Filterings like Wiener filtering, Gaussian filtering, Anisotropic filterings[5,6,7] are deployed. These filtering algorithms involve convolution operations using kernel masks. Later, various techniques are stemmed out to enhance the noise removal. Buades et.al identified the Non-local Means filtering[8]. It calculates the mean value for entire image pixels which is then further weighted to find the similarity between the original and targeted image. Perona et.al[7] introduced an Anisotropic diffusion algorithm, which reduces the image noise and produces the space-variant transformation of the given input image. It aims to preserving the important informations like edges, boundaries etc. It forms a scale space and follows diffusion process. The convolution between the original image and the filter produces the resultant denoised image.

Dabov et.al[9] proposed a 3D transform domain denoising technique using the block-matching concept (BM3D). The image blocks are processed by a sliding window. A 3D array stack is build by accumulating the similar blocks. Applying 3D decorrelating unitary transform on these 3D stacks benefits high correlation exposure. Finally, Shrinkage operator is employed on the transform coefficients to efficiently decrease noises. Aharon et.al.[10] developed a K-Singular Value Decomposition (K-SVD) denoising algorithms using sparse representations. It utilizes dictionary to identify the best representations of the given training data. It is an iterative process which updates the dictionary columns along with the corresponding sparse data coefficients for better data fitting. Therefore, it achieves faster convergence. Gu et.al[13] introduced an image denoising technique named weighted nuclear norm minimization (WNNM). Without knowing the previous understanding of the image, it allows setting of different weights for each singular values. It is developed from Nuclear Norm Minimization (NNM)[14] to prevent data loss by preserving the quality of input image.

## III Methodology:

The proposed work compares the different algorithms for retinal image denoising. The input image is a gray scale SD-OCT images. Initially, the input image is resized to 256x256 images using the imresize operation. This section explains the algorithms which are used to denoising the resized images. The outline of the proposed work is shown in Figure 1.

### 3.1 Speckle Patterns:

Speckle noise can be modelled in mathematical form as follows

$$I(x, y) = m(x, y)n_s(x, y) + n_a(x, y) \quad (1)$$

where  $m(x, y)$  denotes the clean image;  $I(x, y)$  represents the noisy image comprising the components of multiplicative noise  $n_s(x, y)$  and additive noise  $n_a(x, y)$ . Multiple backscattering of light in SD-OCT images induces more multiplicative noise and less additive noise. On that account, the above equation can be redefined as

$$I(x, y) = m(x, y)n_s(x, y) \quad (2)$$

### 3.2 Gaussian Filter:

The Gaussian filter uses the Gaussian distribution function, which is convolving with the input images to obtain the denoised images. It can efficiently reduce the noise level and smoothening the images. The Probability density function  $P(x)$  can be defined as

$$P(x) = \frac{1}{\sqrt{2\pi\sigma^2}} e^{-\frac{(x-\mu)^2}{2\sigma^2}}$$

where input image  $x$  refers the gray scale image,  $\mu$  and  $\sigma$  are the mean and standard deviation respectively.[6]

### 3.3 Anisotropic Diffusion:

Anisotropic diffusion is also known as Perona-Malik diffusion. This filtering technique retains the substantial information of the images while reducing the noises. It abstracts the concept of diffusion and iterative in nature. The output denoised image is produced, involving the convolution of original image with space-variant filters. Hence, the linear structures are preserved along with the smoothening of image. Then anisotropic diffusion is defined as

$$\frac{\partial I}{\partial t} = \text{div}(c(x, y, t)\nabla I) = \nabla c \cdot \nabla I + c(x, y, t)\Delta I$$

Where  $I$  is the Input image,  $\nabla$  and  $\Delta$  refer the gradient and Laplacian operators respectively,  $c(x, y, t)$  is the diffusion coefficient[7].

### 3.4 Non Local Means Filtering:

Non Local Means filtering builds the denoised image by replacing the target pixel with the mean value of similar pixels. As a result, the output image results in better clarity without losing the significant details. Mathematically, NLM can be expressed as

$$u(p) = \frac{1}{C(p)} \int f(d(B(p), B(q))) u(q) dq$$

where  $d(B(p), B(q))$  - Euclidean distance between the point  $p$  and  $q$  of the image[8].

$f$  - decreasing function;  $C(p)$  - normalizing factor.

### 3.5 BM3D:

Block-matching and 3D filtering (BM3D) is an advancement of Non-Local means. It includes two different stages namely Hard thresholding and Wiener filter. Three different operations are performed in these two stages. 1. Grouping: The blocks in the image are processed using a sliding window. The similar image blocks are combined together using the block matching technique. These similar blocks are piled together to create a 3D array. 2. Collaborative Filtering: Filtering is applied on every image block group. A linear transform is applied to manifest the high correlation data. Then Wiener filtering is employed. Again, Inverse linear transformation helps to reconstruct the filtered blocks[9].

### 3.6 K-SVD:

The principle of sparse representation is that, each patch in an image must be modelled as a linear composition of different patches from a comprehensive dictionary. K-SVD algorithm follows dictionary learning method. represent the sparse data, it creates a dictionary using singular value decomposition from both the image and the dataset. It changes the sparse input data and the dictionary atoms repeatedly to find the appropriate data. The optimization problem used to learn the dictionary can be expressed as

$$\arg \min_{x, D, \alpha} \lambda \|y - x\|_2^2 + \sum_i \|R_i x - D \alpha_i\|_2^2 + \sum_i \mu_i \|\alpha_i\|_1$$

where D-Dictionary; y- noisy image;  $x_i$  -patch value from image x with matrix value  $R_i$ [10]

### 3.7 WNNM:

WNNM is an extension of Nuclear Norm Minimization (NNM) and adopts non-local self similarity. A set of similar patches of a particular reference image are gathered and placed in a data matrix. It implements pair wise matching, an efficient grouping technique to compare the similarities between the original and noisy image patches. The distance measure is a useful tool to find the similarities between the image patches. The smaller distance value signifies a higher degree of similarity. Different distance metrics might be used; however the WNNM approach uses the Euclidean distance. The first N patches are grouped as the similar patches, which will ultimately be sorted into a matrix, and WNNM sorts all the similar patches in descending order according to the similarity values. It is expected that the patch matrix is a low rank matrix. Thus, using low rank matrix approximation, a noise-free patch may be restored.

The minimizing cost function for the WNNM problem is

$$\hat{X} = \arg \min_X \|Y - X\|_F^2 + \|X\|_{w,*}$$

where  $\|X\|_{w,*}$  denotes the weighted nuclear norm of X[13]

## IV Experimental Analysis:

### 4.1 Datasets:

The experiments are carried in Duke dataset which consists of SD-OCT images obtained from 45 patients: 15 normal images, 15 Dry AMD images and 15 DME images. These images are captured using Spectralis SD-OCT (Heidelberg Engineering Inc., Heidelberg, Germany) imaging modality[15].

The experiment is carried in Matlab and the performance is assessed for noise levels like 15, 25, 35 and 50 using the different quantitative metrics. The Denoised image output of three SD-OCT images using different algorithms is shown in Table 1. Table 2 exhibits the performance analysis of denoising algorithms for SD-OCT images.

### 4.2 Performance Metrics:

#### *Peak Signal To Noise Ratio (PSNR):*

It measures the image quality of the denoised image. If the value is higher, then the image quality is high.

It can be expressed as

$$PSNR = 10 \log_{10} \left( \frac{MAX_I^2}{MSE} \right)$$

where  $MAX_I$  - maximum value of the input image I

**Structural Similarity Index (SSIM):**

It calculates the structural similarities of the original and denoised image. It can be expressed as

$$SSIM(x, y) = \frac{(2\mu_x\mu_y + c_1)(2\sigma_{xy} + c_2)}{(\mu_x^2 + \mu_y^2 + c_1)(\sigma_x^2 + \sigma_y^2 + c_2)}$$

Where  $\mu_x, \mu_y$  - average value of x and y.  $\sigma_x, \sigma_y$  - variance of x and y and  $\sigma_{xy}$  - covariance of x and y,  $c_1$  and  $c_2$  - constants.

**Normalized Cross Correlation (NK):**

It computes the similarities which has the value in the range [-1 1].

$$NK = \frac{\sum_{i=1}^m \sum_{j=1}^n [I(i, j) - K(i, j)]}{\sum_{i=1}^m \sum_{j=1}^n [I(i, j)]^2}$$

where I and K represents true and denoised image respectively, m,n refers size of the image.

**Normalized Absolute Error (NAE):**

The difference of input image and noise free image sets the value of NAE.

$$NAE = \frac{\sum_{i=1}^m \sum_{j=1}^n |I(i, j) - K(i, j)|}{\sum_{i=1}^m \sum_{j=1}^n |I(i, j)|}$$

where I is the original and K is the obtained image and m,n denotes size of the image.

**Laplacian Mean Square Error (LMSE):**

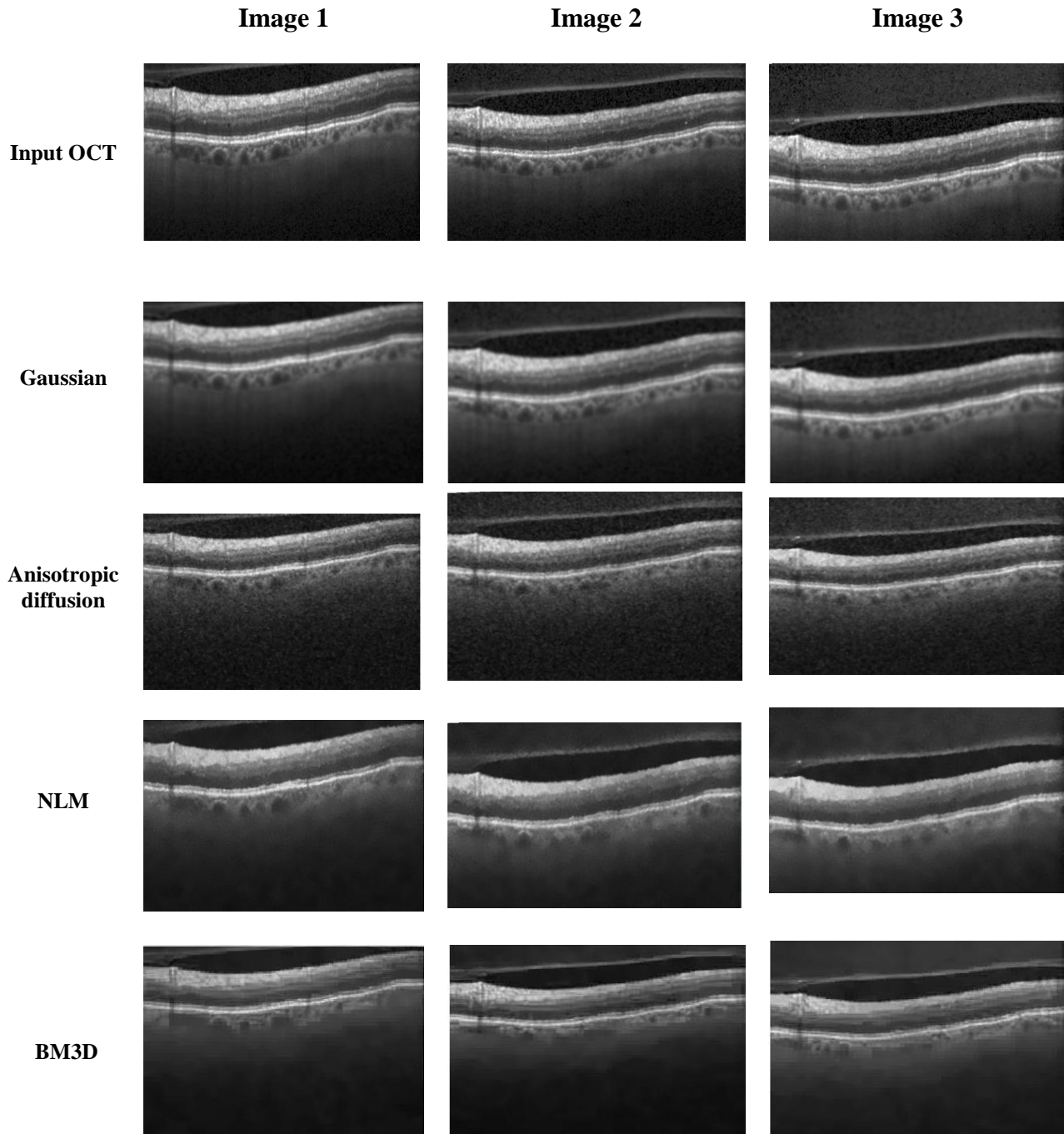
LMSE is obtained by using the Laplacian value of original image and reconstructed image. The lower the value, the higher the quality. Given image I with size mxn and the output image K, LMSE is measured by

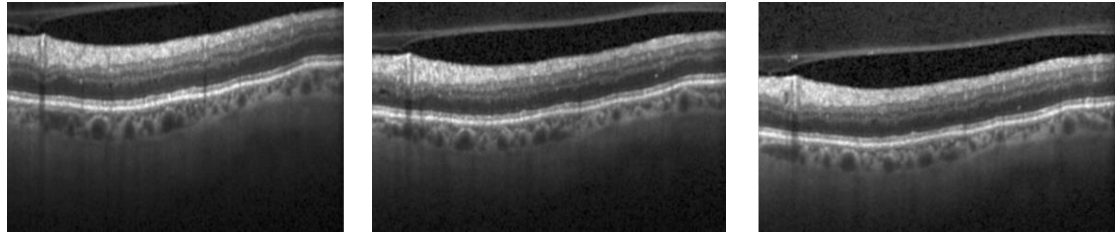
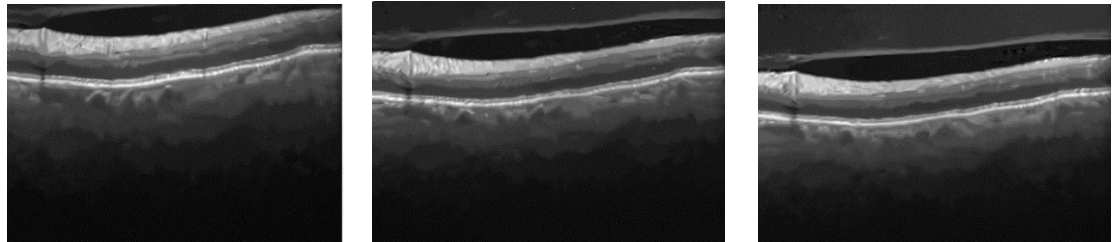
$$LMSE = \frac{\sum_{i=1}^m \sum_{j=1}^n [O\{I(i, j)\} - O\{K(i, j)\}]^2}{\sum_{i=1}^m \sum_{j=1}^n [O\{I(i, j)\}]^2}$$

**Average Difference (AD):**

AD measures the difference between the original and denoised image by considering each pixel value. For image I and the denoised image K with size m x n, AD can be calculated as

$$AD = \frac{1}{mn} \sum_{i=1}^m \sum_{j=1}^n [I(i,j) - K(i,j)]$$



**K-SVD****WNNM****Table 1. Denoised Image Output of three SD-OCT images using different algorithms**

| $\sigma = 15$         |                |               |               |               |               |               |
|-----------------------|----------------|---------------|---------------|---------------|---------------|---------------|
|                       | PSNR           | SSIM          | NK            | NAE           | LMSE          | AD            |
| Gaussian              | 28.7472        | 0.7059        | 0.9894        | 0.3129        | 0.8964        | 7.0658        |
| Anisotropic Diffusion | 28.7958        | 0.7112        | 0.9875        | 0.3347        | 0.9214        | 7.9617        |
| NLM                   | 28.2016        | 0.7118        | 0.9883        | 0.3273        | 0.8938        | 6.8079        |
| K-SVD                 | 29.857         | 0.7225        | 0.9916        | 0.301         | 0.8826        | 5.0356        |
| BM3D                  | 29.9754        | 0.7354        | 0.9919        | 0.324         | 0.8162        | 4.589         |
| WNNM                  | <b>30.6128</b> | <b>0.7542</b> | <b>0.9935</b> | <b>0.1948</b> | <b>0.73</b>   | <b>4.1654</b> |
| $\sigma = 25$         |                |               |               |               |               |               |
| Gaussian              | 27.0699        | 0.6594        | 0.9868        | 0.082         | 0.6819        | 5.5197        |
| Anisotropic Diffusion | 27.2420        | 0.656         | 0.9892        | 0.127         | 0.66216       | 8.7915        |
| NLM                   | 27.5624        | 0.6697        | 0.9905        | 0.1195        | 0.8248        | 8.2745        |
| K-SVD                 | 29.0124        | 0.7134        | 0.9921        | 0.2475        | 0.9314        | 7.8112        |
| BM3D                  | 29.1647        | 0.7424        | 0.9948        | 0.2124        | 0.9238        | 7.7917        |
| WNNM                  | <b>29.7428</b> | <b>0.75</b>   | <b>0.9941</b> | <b>0.2871</b> | <b>0.8792</b> | <b>7.5184</b> |
| $\sigma = 35$         |                |               |               |               |               |               |
| Gaussian              | 26.4926        | 0.5826        | 0.9438        | 0.4286        | 2.3712        | 9.9971        |
| Anisotropic Diffusion | 26.5412        | 0.6054        | 0.9594        | 0.3487        | 2.2547        | 9.9754        |
| NLM                   | 27.0628        | 0.6384        | 0.9621        | 0.3334        | 2.0438        | 9.8397        |
| K-SVD                 | 27.1827        | 0.6467        | 0.9697        | 0.3154        | 1.9484        | 9.1211        |
| BM3D                  | 27.352         | 0.6925        | 0.9689        | 0.2985        | 1.9582        | 9.102         |
| WNNM                  | <b>28.9975</b> | <b>0.7482</b> | <b>0.9734</b> | <b>0.2468</b> | <b>1.9621</b> | <b>8.2417</b> |
| $\sigma = 50$         |                |               |               |               |               |               |
| Gaussian              | 25.1487        | 0.5168        | 0.7627        | 0.5183        | 2.5971        | 11.6724       |



|                       |                |               |               |               |               |               |
|-----------------------|----------------|---------------|---------------|---------------|---------------|---------------|
| Anisotropic Diffusion | 25.1548        | 0.5012        | 0.8164        | 0.4910        | 2.4318        | 10.8975       |
| NLM                   | 25.5975        | 0.5126        | 0.8343        | 0.4726        | 2.3831        | 10.8297       |
| K-SVD                 | 25.6027        | 0.4989        | 0.8368        | 0.4612        | 2.2158        | 10.6975       |
| BM3D                  | 25.9287        | 0.5974        | 0.8847        | 0.4216        | 2.1410        | 9.9472        |
| WNNM                  | <b>26.9875</b> | <b>0.6084</b> | <b>0.9528</b> | <b>0.3574</b> | <b>1.5287</b> | <b>9.4128</b> |

Table 2. Performance analysis of denoising algorithms for SD-OCT images

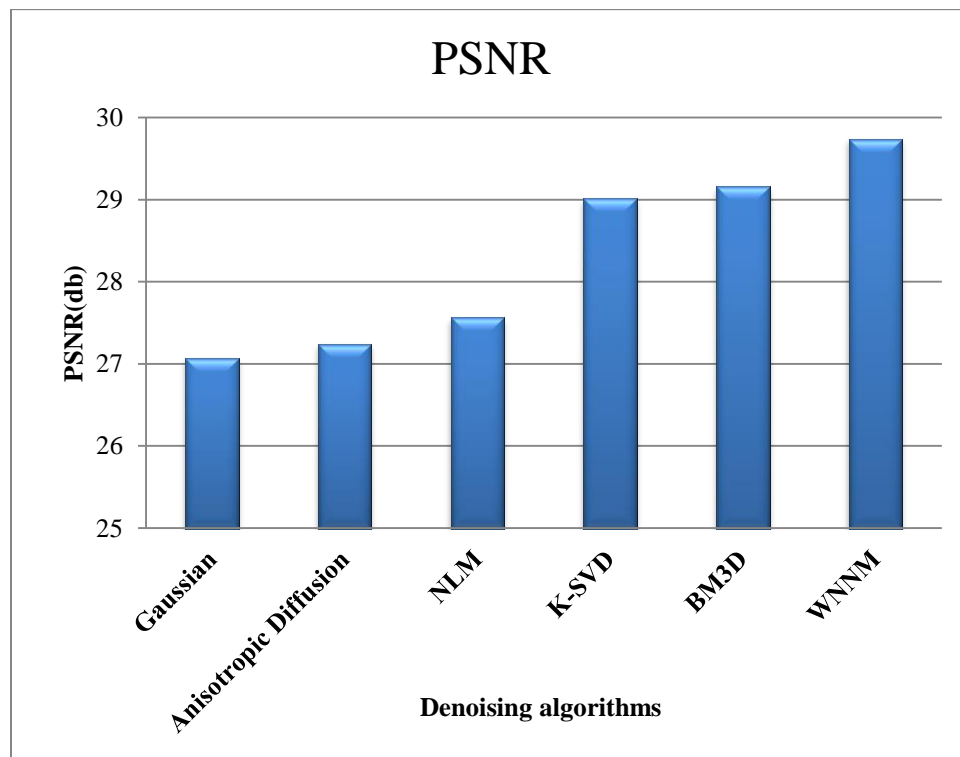


Figure 2. Graphical representation of PSNR value for different algorithms

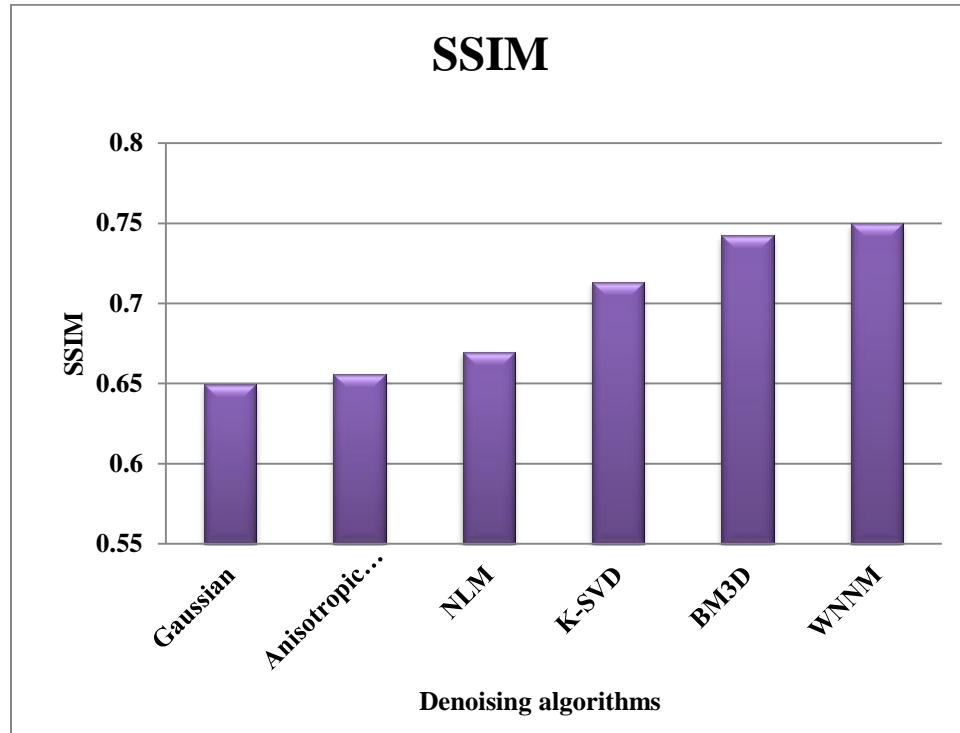


Figure 3. Graphical representation of SSIM value for different algorithms

#### V Conclusion:

The SD-OCT images are corrupted by inherent speckle granules which degrades the image quality. Hence, it is crucial to remove these noises for disease identification. The proposed work illustrates the execution and validation of several noise reducing techniques for speckle reduction in SD-OCT images. The algorithms used here can remove the noises efficiently but the image quality is not retained by all. From the observation, it is obtained that WNNM shows better denoising and preserve the image textures. The quantitative analysis is also conducted using different metrics and it reveals that WNNM has considerable PSNR and SSIM values. In the future work, the investigation on deep learning algorithms will be entailed to achieve significant performance without manual parameter tuning.

#### References:

1. M. Schmitt, "Optical coherence tomography (OCT): a review," in *IEEE Journal of Selected Topics in Quantum Electronics*, vol. 5, no. 4, pp. 1205-1215, July-Aug. 1999, doi: 10.1109/2944.796348
2. Fujimoto, J. G., Brezinski, M. E., Tearney, G. J., Boppart, S. A., Bouma, B., Hee, M. R., ... & Swanson, E. A. (1995). Optical biopsy and imaging using optical coherence tomography. *Nature medicine*, 1(9), 970-972
3. Schmitt, J. M., Xiang, S. H., & Yung, K. M. (1999). Speckle in optical coherence tomography.
4. Jain AK (1989) Fundamentals of digital image processing. Prentice-hall, Inc, Upper Saddle River
5. Benesty J, Chen JD, Huang YT (2010) Study of the widely linear wiener filter for noise reduction. In: Abstracts of IEEE international conference on acoustics, speech and signal processing, IEEE, Dallas, TX, USA, pp 205–208. <https://doi.org/10.1109/ICASSP.2010.5496033>

6. R.A. Haddad and A.N. Akansu, "A Class of Fast Gaussian Binomial Filters for Speech and Image Processing," *IEEE Transactions on Acoustics, Speech, and Signal Processing*, vol. 39, pp 723-727, March 1991.
7. Perona, P., & Malik, J. (1990). Scale-space and edge detection using anisotropic diffusion. *IEEE Transactions on pattern analysis and machine intelligence*, 12(7), 629-639.
8. Buades, A., Coll, B., & Morel, J. M. (2005, June). A non-local algorithm for image denoising. In *2005 IEEE Computer Society Conference on Computer Vision and Pattern Recognition (CVPR'05)* (Vol. 2, pp. 60-65). IEEE.
9. Dabov, K., Foi, A., Katkovnik, V., & Egiazarian, K. (2006, February). Image denoising with block-matching and 3D filtering. In *Image Processing: Algorithms and Systems, Neural Networks, and Machine Learning* (Vol. 6064, p. 606414). International Society for Optics and Photonics.
10. Aharon, M., Elad, M., & Bruckstein, A. (2006). K-SVD: An algorithm for designing overcomplete dictionaries for sparse representation. *IEEE Transactions on signal processing*, 54(11), 4311-4322.
11. Mairal, J., Bach, F., Ponce, J., Sapiro, G., & Zisserman, A. (2009, September). Non-local sparse models for image restoration. In *2009 IEEE 12th international conference on computer vision* (pp. 2272-2279). IEEE.
12. Dong, W., Zhang, L., Shi, G., & Li, X. (2012). Nonlocally centralized sparse representation for image restoration. *IEEE transactions on Image Processing*, 22(4), 1620-1630.
13. Gu, S., Zhang, L., Zuo, W., & Feng, X. (2014). Weighted nuclear norm minimization with application to image denoising. In *Proceedings of the IEEE conference on computer vision and pattern recognition* (pp. 2862-2869).
14. Fazel, M. (2002). Matrix rank minimization with applications. PhD thesis, Stanford University.
15. Srinivasan, P. P., Kim, L. A., Mettu, P. S., Cousins, S. W., Comer, G. M., Izatt, J. A., & Farsiu, S. (2014). Fully automated detection of diabetic macular edema and dry age-related macular degeneration from optical coherence tomography images. *Biomedical optics express*, 5(10), 3568-3577.
16. Eskicioglu, A. M., & Fisher, P. S. (1995). Image quality measures and their performance. *IEEE Transactions on communications*, 43(12), 2959-2965.
17. Wang Z, Bovik AC, Sheikh HR, Simoncelli EP (2004) Image quality assessment: from error visibility to structural similarity. *IEEE Trans Image Process* 13(4):600–612.
18. Hore A, Ziou D (2010) Image quality metrics: Psnr vs. ssim. In: 2010 20th international conference on pattern recognition (icpr), IEEE, pp 2366–2369